11

The Use of PEEK in Spine Arthroplasty

T. Brown[1], Qi-Bin Bao[1] and Hansen A. Yuan[2]
[1]*Pioneer Surgical*
[2]*SUNY Upstate, New York*
USA

1. Introduction

Cervical and lumbar disc arthroplasty are one component in the continuum of treatment for symptomatic degenerative disc disease (DDD) that is unresponsive to conservative care. In the lumbar spine, this may be accomplished via nucleus replacement or total disc replacement, and in the cervical spine by total disc replacement. The goal of both lumbar disc arthroplasty treatments are the same; relieving discogenic back pain through removing the pain source and restoring or maintaining motion segment function. For cervical arthroplasty, the goal is to relieve radicular pain as a result of nerve root compression, and/or myelopathy as a result of spinal cord compression, in addition to preserving motion. From a design standpoint, nucleus replacement technology consists of elastomers and non-elastomers, both preformed and *in-situ* cured, and can incorporate articulation similar to total disc replacements, with the intent of replicating to various extents the natural nucleus and preserving most of the annulus, thereby relying on a biomechanically intact annulus to share the compressive load. Also, most artificial nucleus devices are not fixed to the vertebral endplates, and therefore allow small, relative motion between their external surfaces and the vertebral endplates. In contrast, the majority of total disc replacement technology consists of articulating designs and material combinations that have been developed based upon the wealth of scientific and clinical information produced by the success of total joint arthroplasty. An artificial disc is designed to replace the entire disc tissue by excising almost all the disc materials, and therefore removing all the natural constraints in the anterior column. In addition, all artificial discs have a superior plate and an inferior plate, which are fixed to the two adjacent vertebrae. These represent key design differences between the two technologies.

A key challenge for a disc arthroplasty device is selecting the proper material(s) for the various components that consitute its design. Unlike total joint replacement, a candidate for disc arthroplasty is on average 40 years of age with a target indication of 18 to 60 years (Zigler et al., 2007; Murrey et al., 2009). As a consequence, these devices are expected to last much longer than those of total joint recipients, whose average age is 70 years (Bergen, 2011, Garellick et al., 2010). Therefore, there are stringent requirements for long term implantable materials, and this will significantly limit the selection of materials available. Biocompatibility and biodurability, otherwise known as the abilities of a material to maintain its physical and chemcial integrity under *in vivo* applications without eliciting an aggressive host immune response for a given application, are essential for permanent

medical implants. Since a central tenet of all arthroplasty devices is the preservation of motion, it is therefore expected that these devices will produce wear particulate, and the subsequent potential biologic activity needs to be evaluated. This is in addition to exhibiting sufficient strength and fatigue performance over the expected lifetime of the device within the *in vivo* environment. Subsequently, disc arthroplasty devices should be introduced into clinical use only after a successful preclinical evaluation of their mechanical and biological properties within the scope of their intended use, as failure can lead to a technically challenging revision, increased economic burden and more importantly, a significant risk to the patient (Devin et al., 2008, Cavanaugh et al., 2009, Francois et al., 2007, Guyer et al. 2011, Lucina & Thorpe, 2004, Punt et al., 2009).

Initially, much of the preclinical testing of candidate materials is not conducted on the device but rather the material itself. Logical progression then leads to testing of the device itself, since the design of the device will also affect a given materials performance. These tests should include bench top testing such as static and fatigue assessments, wear testing, and evaluation in human cadaver and animal models. The wear, mechanical durability and potential resultant biologic activity of disc arthroplasty devices are a key component that needs to be addressed prior to clinical use. This can be assessed to a large extent by the appropriate wear tests for articulating devices and fatigue tests in the case of devices that utilize elastomers for the basis of their motion. However, in the absence of significant implant retrievals, the appropriate tests to perform in assessing a respective devices' durability properties becomes critical. Device fatigue and wear may decrease the devices' lifespan for its intended application. In addition, the wear particulate generated may result in a particle mediated inflammatory response potentially leading to osteolysis or delayed type hypersensitivity. Evaluation of the particulate generated can allow for assessment of potential biologic reactivity. Successful animal models can act as a final spring board for initiation of clinical studies by evaluation of the mechanical behavior and elicited histopathological response of the device component materials following long-term implantation. Analyses can based upon gross necropsy, MRI radiography, plain X-ray, microradiography, multi-directional flexibility testing and biocompatibility assays (local and systemic histology). The overall successful completion and evaluation of these studies allows for advancement to the clinical stage.

Traditionally metal alloys, ceramics and polymers have been the materials of choice for arthroplasty applications. Ceramics are noted for their high wear resistance and strength, and metal alloys, such as titanium (Ti) and cobalt chrome (CoCr) for their high strength, fracture toughness and hardness; properties that are necessary for long term implantable materials. Polymers are a more compliant material, with low-friction properties ideal for articulating surfaces which produce relatively inert wear debris. These materials and combinations thereof have a long clinical history in total joint arthroplasty. Therefore, material combinations such as metal on UHMWPE and metal on metal are typically used for articulating disc replacements based upon the established scientific and clinical history of these bearing couples in total joint arthroplasty. Poly-ether-ether-ketone (PEEK) is a linear, aromatic thermoplastic with proven biocompatibility and biostability. It can be repeatedly steam and gamma sterilized with no detrimental effects on its bulk material properties. It is an exceptionally strong engineering thermoplastic that retains its mechanical properties even at very high temperatures (Rae, 2007). The material is tough and abrasion resistant with high-impact strength and excellent flexural and tensile properties. It has a low coefficient of friction and resists attack by a wide range of organic and inorganic chemicals and solvents. To this end, PEEK is widely used in the lumbar spine for both fusion

(Rousseau et al., 2007) and non-fusion applications (Balsano, 2011; Senegas, 2002) due to its excellent mechanical strength, biostability, biocompatibility and radiolucency (Kurtz & Devine, 2007), and has replaced to a significant extent the use of metallic cages. It is also commonly used in the cervical spine in the form of interbody cages for fusion. Therefore, it potentially has most of the material characteristics deemed to be required for use as material in spine arthroplasty applications. However, unlike traditional polymers and metals, common materials used in the spine arthroplasty arena, the use of PEEK represents a new material for disc arthroplasty applications in the cervical and lumbar spine, and as such, its use as a material for this technology has largely gone unexplored.

PEEK has recently been used in the form of a nucleus replacment device and in the form of a cervical total disc replacement. Both devices utilize a ball and socket articulation for motion. As part of evaluating the safety and effectiveness profile of both devices, several preclinical tests were successfully performed to satisfy FDA and the Essential Requirements of the Medical Device Directive (MDD) for CE mark requirements prior to clinical use. Each device is CE marked and currently in clinical use. Worldwide clinical results as measured by validated measures such as Oswestry Disability Index (ODI), Visual Analog Scale (VAS), along with patient satisfaction, suggest that both devices can relieve the symptoms of their respective degenerative processes, with no adverse events occurring as a direct result of the device not performing as expected from a biomaterial perspective. The methodology, results and interpretation of these preclinical studies that have allowed for advancement to the clinical stage will be discussed, along with the clinical results in light of both devices' clinical performance.

2. Preclinical studies and results

2.1 PEEK cervical total disc replacement device

The cervical arthroplasty device incorporates a unique, Ti cam blade fixation system that can be described as a rotating shaft with blades for primary fixation (Figure 1). Given that PEEK is a relatively bio-inert material, bone apposition does not readily occur onto the material. Therefore, a plasma-sprayed hydroxyapatite (HA) coating was added to the outer endplates. The design objectives are to achieve secure, long term fixation within the disc space, exhibit the necessary strength and durability for the lifetime of the patient for its intended use, and restore or maintain the range of motion (ROM) at the operative level while simultaneously not adversely affect the biomechanics at the adjacent levels.

Fig. 1. PEEK cervical arthroplasty device.

2.1.1 Axial static and fatigue strength

To determine the static and fatigue strength of the device, the smallest footprint (12x14 mm) and height (5 mm) was utilized. Testing was performed on an MTS 858 Mini-Bionix II test frame with the devices mounted on steel fixtures. A comparison was made between HA coated devices and uncoated devices to determine if the coating had an adverse effect on the static and fatigue strength of the device. A sample size of 6 was used for the static test with a displacement rate of 2 mm/min. The acceptance criteria was an offset yield load of greater than 1200 N for the axial static testing. For the fatigue tests, a sample size of 2 was used with a starting fatigue load of 75% of the static offset yield load of the uncoated devices, with R=10 at 10 Hz.

For the axial static testing, the results showed that the mean load at offset yield was calculated to be 7,631 ± 171 N at a displacement of 0.50 ± 0.01 mm for the uncoated devices and 9640 ± 251 N at a displacement of 0.70 ± 0.02 mm for the coated devices, which was significantly greater (t-test, $p<0.001$). The primary mode of failure in the tested constructs was fracture of the PEEK. For the axial fatigue testing, the uncoated and coated samples reached 10 million cycles at a load of 5723 N (R=10). No evidence of failure, such as fatigue cracks or gross deformation, was seen during the inspections or after test. When the coated devices were tested at a load of 7230 N, implant fracture occurred at 867,966 cycles.

The literature suggests that the maximum compressive load on the cervical spine during the performance of physical tasks is 1.2 kN [Moroney, 1988] and that the elastic limit of single motion segments could be as high as 1.23 kN, with a predicted ultimate compressive strength of 2.40 kN [Przybyla, 2007]. The results showed that the loads reached were significantly above the expected *in vivo* loads of the cervical spine, and that the HA coating did not negatively affect the axial compressive static or fatigue performance.

2.1.2 Shear static and fatigue strength

To determine the shear static and fatigue strength of the device, the smallest footprint (12x14 mm) and height (5 mm) was utilized. Testing was performed on an MTS 858 Mini-Bionix II test frame with the devices mounted on steel fixtures. According to the literature, the total ROM for flexion/extension of the cervical spine is greatest at the C_4-C_5 level, and appears to be slightly more than 20° when measured *in viv*o using computer assisted tracking software [Reitman, 2004]. The literature also shows that the amount of mean flexion is only slightly higher than the mean extension [Panjabi, 2001]. Therefore, the shear test was conducted at 10° for both flexion and extension. A comparison was made between HA coated devices and uncoated devices to determine if the coating had an adverse effect on the shear static and fatigue strength of the device. A sample size of 6 was used for the static tests with a displacement rate of 2 mm/min. The acceptance criteria was an offset yield load of greater than 135 N [Moroney, 1988] for the shear static testing and for the fatigue tests, a sample size of 2 was used with a run out load greater than 135 N [Moroney, 1988] with R=10 at 10 Hz.

For the shear static testing at 10° flexion, the mean load at offset yield was calculated to be 4774 ± 372 N at a displacement of 0.44 ± 0.01 mm. For the shear static testing at 10° extension static shear, the mean load at offset yield was calculated to be 6788 ± 412 N at a displacement of 0.53 ± 0.02 mm. The primary mode of failure was fracture of the PEEK (Figure 2). Since the results of the static compressive shear strength resulted in a lower offset yield load in flexion (4744 N) versus extension (6788 N), the fatigue test was run at 10° flexion as a worst case scenario. The results of the fatigue testing at 1600 N showed the

devices reached 10 million cycles without experiencing any visible plastic deformation or fracture. For the coated devices, since the shear static loading was significantly higher than the acceptance criteria and the coating was shown to not have a detrimental effect on the axial static properties of the device, only shear fatigue testing was performed. The results were the same as the coated devices, 1600 N of compressive shear to 10 million cycles without experiencing any visible plastic deformation or fracture. Therefore, it was concluded that shear fatigue loads can be withstood far beyond those that would be expected *in vivo*.

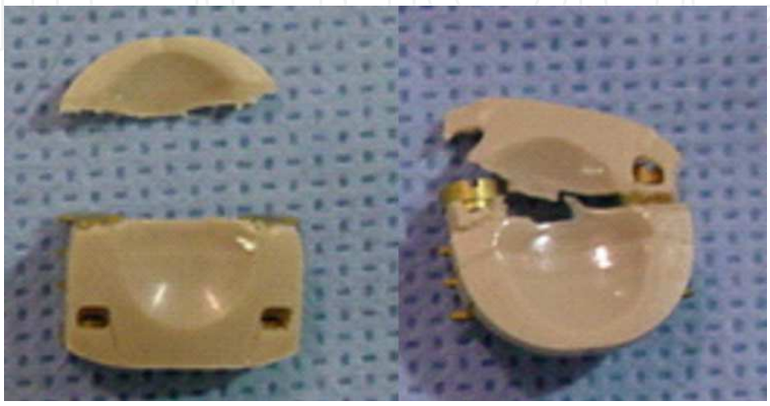

Fig. 2. PEEK cervical arthroplasty device after static compressive shear testing to failure. Left – tested under 10° flexion, right – tested under 10° extension.

2.1.3 Fixation strength

The fixation strength of the device was assessed by determining its pull out strength using a synthetic vertebral model. The largest (17x17 mm) and smallest footprints (12x14 mm) of 8 mm height were utilized. To avoid the variability produced by human cadaveric tissue, including bone mineral density and endplate geometries, a synthetic fixation medium of ASTM grade 15 polyurethane foam was selected for use. The fixation pull out test model consisted of compressing the device between two polyurethane blocks to 60 lbs, and then performing a uniaxial tensile load to failure test, thereby forcibly removing the implant. The test was conducted on an MTS 858 Mini-Bionix II test frame with appropriate fixturing. The displacement rate was 2.5 mm/sec. The implant was placed between the blocks in accordance with the surgical technique. A minimum of ten pullout tests were performed for each implant size. This data was then compared to eight previously tested cervical disc arthroplasty devices used clinically in cervical reconstruction that utilize press fit, keel or screw fixation using the same test protocol and laboratory [Cunningham, 2010]. Therefore, the results of this testing provides for a standardized testing methodology to quantify the strength of fixation and resistance to migration.

In all pullout tests for the two implant sizes, there was no incidence of intrinsic device failure. Failure always occurred at the polyurethane block-implant interface. The cam blade fixation indicated the highest pullout strength, which was statistically different from nearly all other designs (Table 1). Prosthetic endplates containing toothed ridges and keel fixation ranked next in terms of fixation strength. Although intuition favored the coronal keel as affording an increased mechanical advantage over the toothed surface, there were no

observed statistical differences in pullout strength between the two endplate designs ($p>0.05$). In fact, the toothed surfaces indicated a slightly higher failure load over the keel device, although not statistically different. Moreover, the utilization of toothed ridges

Experimental Group	Device Fixation Type	Endplate Surface Area (mm^2)	Failure Load (N)
PEEK cervical device (small)	Cam blade	168	386.3 ± 44.1*
PEEK cervical device (large)	Cam blade	289	566.2 ± 72.0**
PCM Low Profile	0.2 mm endplate serrations	300	257.4 ±28.5
PCM V-Teeth	0.2 mm endplate serrations with 1.0 mm toothed ridges	300	308.8 ± 15.3
PCM Modular Flange	Serration with (4) 4 mm x 15 mm screws	300	496.4 ± 40.0
PMC Fixed Flange	(4) 4 mm x 15 mm screws	300	528.0 ± 127.8
Prestige LP	2.3 mm height center keel with teeth	275	306.4 ± 31.3
Kineflex C	0.2 mm endplate serrations with 2.5 mm height center keel	250	286.9 ± 18.4
Anterior Cervical Plate with Interbody Cage	Serration with 4 screws	180	635.5 ± 112.6
Iliac Crest Autograft	N/A	235	161.6 ± 16.6

Table 1. Fixation strength of the PEEK cervical arthroplasty device as compared to other forms of fixation. * Fixation strength was significantly greater than all others with the exception of PCM Fixed Flange and Anterior Cervical Plate with Interbody Cage. **Fixation strength was significantly greater than all others with the exception of PCM Fixed and Modular Flange, Prestige LP and Anterior Cervical Plate with Interbody Cage. There were no statistical differences between endplate surface areas.

elevated beyond 1.0mm did not significantly improve fixation strength ($p>0.05$). Prosthetic endplates containing serrated edges (0.2mm) alone indicated the lowest fixation strength. These results indicate not only a high fixation strength but the ability of the PEEK housing for the cam blades to withstand the expected *in vivo* shear forces placed upon the device.

2.1.4 Wear testing and wear particulate characterization

Wear testing was performed on six devices of the smallest footprint (12x14 mm) and 5 mm height using an MTS Spine Wear Simulator. The test parameters consisted of ASTM F2423-05 recommended multidirectional motion and static load profiles from 0-10 million cycles followed by ISO 18192-1 recommended motion and dynamic load profiles from 10-20 million cycles. The test frequency was 2 Hz for motion and 4 Hz for load. The testing fluid consisted of newborn calf serum diluted with phosphate buffered saline (PBS) to a final protein content of 20 g/L. Ethylene-diamine tetraacetic acid (EDTA) was added to the serum at a concentration of 20 mM to bind the calcium ions present in the serum. EDTA is a known preservative, and together with the low protein content and PBS, the addition of sodium azide or other anti-bacterial agent was not used. The test fluid temperature was kept at 37 ± 3° C. Unloaded soak controls were used to account for moisture uptake. After 0.5 million cycles, the tests were stopped at 1 million cycles and at million-cycle intervals thereafter to clean, dry and gravimetrically assess the wear rates. The test fluid was subsequently collected and stored at -20° C. The average wear rates were determined using linear regression analysis with one-way-analysis-of-variance (ANOVA) used to determine if significant differences ($p < 0.05$) in the wear rates between methodologies were present. Complimentary to the wear testing, particle analysis was performed using light scanning electron microscopy (SEM). The proteinacious test serum containing PEEK wear debris underwent enzymatic digestion (5x Trypsin digestion and 1.5 mg/mL of Proteinase K per sample at 37° C for 24 hours) followed by a mild acid treatment (10% HCl at 37° C for 24 hours), meeting or exceeding similar protocols previously established to be equivalent for acid and base digestion (Niedzwiecki, 2001). The particles were then analyzed by SEM analysis and characterized according to their equivalent circle diameter (ECD), aspect ration (AR), roundness (R) and form factor (FF) in accordance with ASTM F 1877-05.

All implants maintained full functionality throughout each test duration. The results showed only a slight, non-significant variation in the wear rates over the course of 20 million cycles. The wear rate for the first 10 million cycles was approximately 0.26 ± 0.01 mm^3/million cycles. For the interval of 10 to 20 million cycles, the wear rate increased slightly, 0.32 ± 0.02 mm^3/million cycles. These wear rates are similar to other arthroplasty devices in clinical use (Figure 3). Although the wear rates were relatively consistent, the particle size was sensitive to the test method. The particle analysis revealed that the size (ECD) of the particulate was larger for the ISO testing methodology (2.56 μm) as compared to the ASTM methodology (1.67μm) (Figure 4). However the particle morphology, an equally important parameter influencing biological activity, was similar for both methods. The ASTM testing revealed a smaller particulate; however it may be unlikely that a static compressive load occurs in the cervical spine *in vivo*, since the literature suggests that a dynamic compressive load occurs due to muscle contraction during kinematic activities [Snijders, 1991].

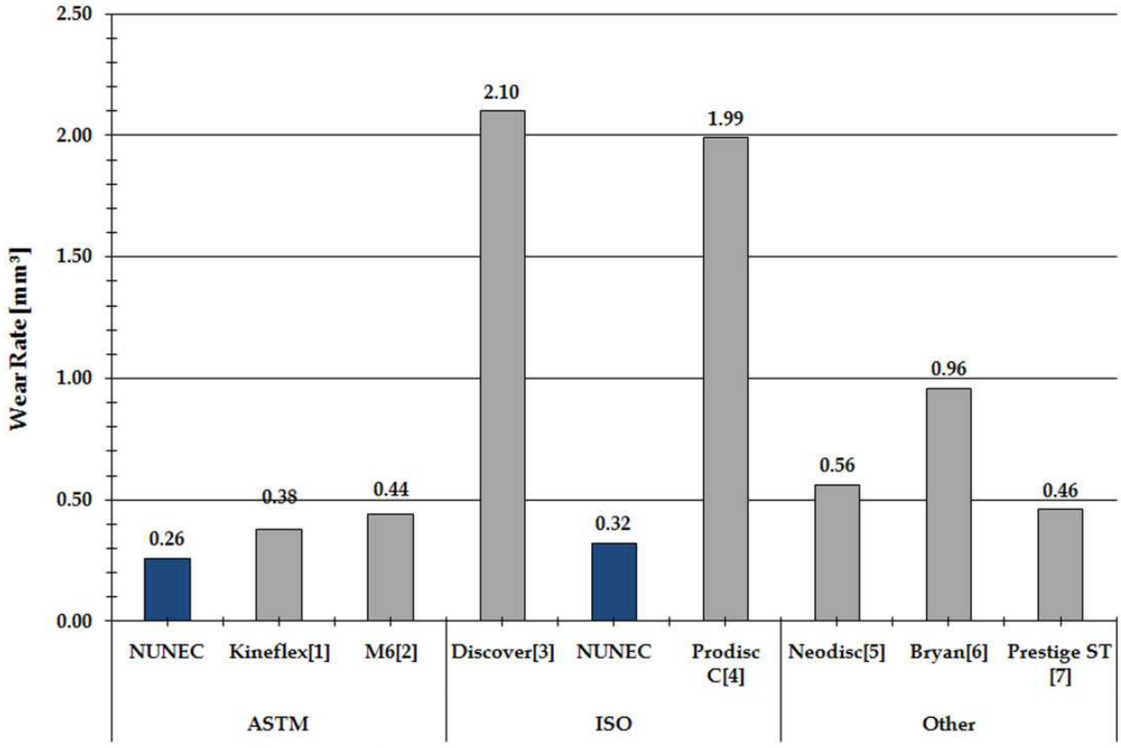

Fig. 3. Wear rate comparison of the PEEK cervical arthroplasty device to other devices in clinical use.

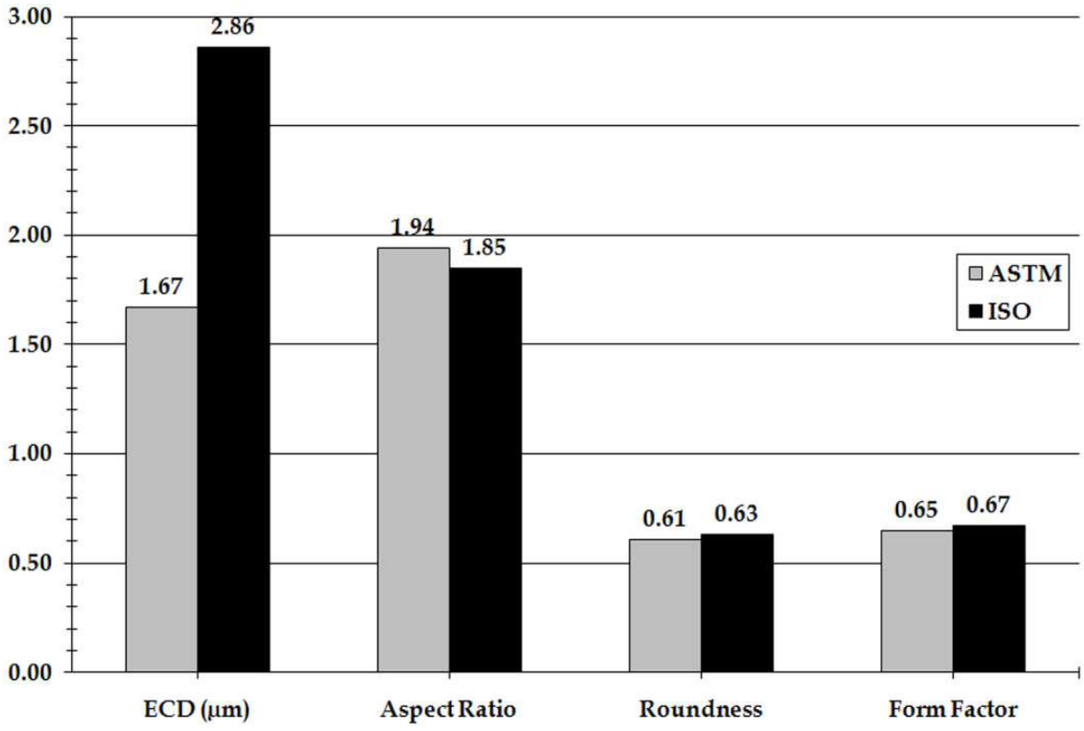

Fig. 4. SEM analysis of the PEEK particulate generated from the wear tests.

Methodology	Group 1- Normal Load	Group 2 - Artificially Aged	Group 3 – High Load
Environmental Condition			
Sterilization	30 kGy in air	200 kGy in air	30 kGy in air
Aging	N/A	Exposure to O_2 at 70° C for 40 days	N/A
Dynamic Compressive Load	225…1024 N	225…1024 N	200…2000 N
Motion	ISO - 6°/3° flexion/extension ±2° lateral bending and axial rotation to 10 million cycles	ISO - 6°/3° flexion/extension ±2° lateral bending and axial rotation to 10 million cycles	ISO - 6°/3° flexion/extension ±2° lateral bending and axial rotation to 10 million cycles
Test Frequency	Compressive Load 4 Hz Motion 2 Hz	Compressive Load 4 Hz Motion 2 Hz	Compressive Load 4 Hz Motion 2 Hz

Table 2. Summary of Testing Methodology for All Groups.

2.1.5 Hydroxyapatite coating and substrate effects

The HA coating is applied to the outer endplates of the device via the well known plasma spray process. The coating was characterized in accordance with FDA guidelines. Given that the device' material (PEEK) is being exposed to what is considered a high temperature process, a potential change in the materials biocompatibility profile and/or material properties could occur. Therefore, several tests were performed to ensure that the thermal and chemical signature of the PEEK substrate was not adversely affected. This consisted of Differential Scanning Calorimetry (DSC), Thermal Gravimetric Analysis (TGA) and Fourier Transform Infrared Spectroscopy (FTIR), the most common tools used to characterize polymers. This was then compared with the 20-year historical measurements of PEEK provided by the manufacturer (Invibio). Analyses were performed on bulk and surface samples.

For the DSC, TGA and FTIR analysis, six machined samples of HA coated PEEK that subsequently had the coating removed by a 10% phosphoric acid treatment were compared to machined PEEK samples that had not been coated. The DSC analysis showed similarity between all samples and to machined PEEK samples. Likewise, ATR-FTIR showed no appreciable difference in the tested samples. TGA analysis resulted in primary degradation of the samples starting at approximately 550°C and continuing until about 625°C, showing an initial degradation loss of 35%. There was a dramatic decrease in sample mass (65% of the initial mass down to 0% of the initial mass) of the samples between 625° C and 800° C. There was no appreciable difference in the samples, and the degradation response looked very similar to the machined PEEK samples. All observed values (mean, maximum and minimums) were within the 20 year historical ranges of PEEK as verified by Invibio. More importantly, from a biocompatibility standpoint, since there were no additional absorption peaks found in the regions that formerly had an HA coating, and the HA coating was

readily removed with a mild solvent, it is highly unlikely that any covalent bonding occurred between the HA and the PEEK material. Furthermore, there was no measurable change in the molecular structure of the PEEK induced by adding the HA layer. Therefore, no chemical bonding was noted to occur, the surface properties and subsequently the biocompatibility profile of the PEEK substrate have not changed, and it can be concluded that only a mechanical bond exists between the PEEK and HA coating.

Biocompatibility tests in accordance with ISO 10993 parts 5, 10 and 11 were conducted at NAMSA. These tests were carried out on coated and an equal number of substrates having the coating removed with a mild solvent (phosphoric acid) in order to expose the underlying substrate. The control consisted of virgin PEEK:

ISO 10993, Part 5: Tests for Cytotoxicity-

HA coated PEEK and coated PEEK that had the coating removed, were prepared using single strength Miminum Essential Medium supplemented with 5% serum and 2% antibiotics (1X MEM). The test extracts were placed onto three separate monolayers of L-929 mouse fibroblast cells propagated in 5% CO_2. Three separate monolayers were prepared for the reagent control, negative control and for the posititve control. All monolayers were incubated at 37° C in the presence of 5% CO_2 for 48 hours at which point they were examined microscopically to determine any change in cell morphology. Under the conditions of this study, the 1X MEM test extract showed no evidence of causing cell lysis or toxicity. The reagent control, negative control and the positive control performed as anticitpated. Therefore the requirements of the study were met.

ISO 10993, Part 10: Test for Irritation and Delayed-Type Hypersensititivity-

A guinea pig (Hartley albino) maximization test was conducted to evaluate the potential for delayed dermal contact sensitization. HA coated PEEK and coated PEEK that had the coating removed, were extracted in 0.9% sodium chloride USP solution (SC) and sesame oil, NF (SO). Each extract was intradermally injected and occlusively patched to ten test guinea pigs per extract in an attempt to incude sensitization. Five additional guinea pigs served as a control. All sites were scored at 24 and 48 hours after patch removal. HA coated PEEK and coated PEEK that had the coating removed, were extracted in 0.9% sodium chloride USP solution (SC) and sesame oil, NF (SO). A 0.2 mL dose was injected by the intracutaneous route into five separate sites on the right side of the the back of two New Zealand white rabbits. Similarly, the corresponding control was injected on the left side of the back of each rabbit. Observations for erythema and edema were conducted at 24, 48 and 72 hours after injection. Under the conditions of this study, there was no evidence of the extracts causing delayed dermal contact sensitization in the guinea pigs or no erythema or edema from the extracts injected intracutaneously into the rabbits. The requirements of the study were met.

ISO 10993, Part 11: Tests for Systemic Toxicity-

HA coated PEEK and coated PEEK that had the coating removed, were extracted in 0.9% sodium chloride USP solution and sesame oil, NF. A single dose of the extract was injected into five mice per extract by either the intravenous or intraperitoneal route. Five mice served as a control. The animals were observed immediately and at 4, 24, 48 and 72 hours after injection. Under the conditions of this study, there was no mortality or evidence of systemic toxicity from the extracts, and therefore the requirements of the study were met.

2.1.6 Biomechanical analysis

Using an *in-vitro* human cadaveric model, the range of motion (ROM) of the device was evaluated at a single level, with data analysis based on the resulting operative and adjacent level multidirectional flexibility properties. A total of twelve fresh-frozen human cadaveric cervical spines (C_1T_3) were harvested en-bloc and utilized. Prior to biomechanical analysis, standard anteroposterior and lateral plain films were obtained to exclude specimens demonstrating intervertebral disc or osseous pathology. In preparation for biomechanical testing, the specimens were thawed to room temperature and cleaned of all residual musculature, with care taken to preserve all ligamentous attachments and facet joint capsules. The proximal (C_1C_3) and distal (T_1T_3) ends of the specimen were stabilized in metal tubing containers using four, four point compression screws. An optoelectronic motion measurement system (3020 Optotrak System) was used for kinematic analysis under a pure moment loading to evaluate the flexion/extension, lateral bending and axial rotational response after reconstruction of the C_4C_5 cervical level. A comparision was made between the intact, destabilized, reconstructed and fusion procedures.

Flexion/extension testing demonstrated the diskectomy condition as producing a five degree increase (10.5 to 15.6°) in operative level range of motion compared to the intact spine and was statistically greater than intact and anterior plate-cage groups ($p<0.05$). Implantation of the PEEK cervical artificial disc restored motion to near intact level (11.9°) which was not statistically different from the intact spine (10.5°) ($p > 0.05$). The final reconstruction using the anterior plate-cage decreased the mean range of motion to 8.71° at the operative level, which resulted in significantly less range of motion than the PEEK artificial disc (11.9°) ($p<0.05$) but not intact condition (10.5 dg) ($p>0.05$). The elevated mean range of motion value for this reconstruction is attributable to the segmental instability created by the diskectomy condition (ANOVA $F=3.72$, $p=0.018$). Biomechanical testing in lateral bending loading did not reveal any significant differences in range of motion when comparing the intact spine and three treatment groups ($p>0.05$). Diskectomy (7.63°), PEEK artificial disc (6.90°) or anterior plate-cage construct (6.77°) afforded a statistical change in flexibility compared to the native intact condition (7.10°). The high standard deviation in the range of motion account for the lack of statistical significance under this loading modality (ROM: ANOVA $F=0.58$, $p=0.633$). Biomechanical testing in axial rotation indicated no statistical differences in ROM between the intact spine, diskectomy, PEEK total disc replacement or anterior plate-cage group ($p>0.05$). The cervical disc replacement procedure (7.21°) resulted in a slight increase in operative level flexibility relative to the intact (6.05°) and diskectomy conditions (6.44°) ($p>0.05$). The trends under this biomechanical loading mode failed to reach statistical significance secondary to specimen variability and high standard deviations. (ROM: ANOVA $F=0.22$, $P=0.882$). Despite the use of the Panjabi Hybrid testing protocol, there were very minimal changes in adjacent level ROM when comparing the intact spine, diskectomy condition and two reconstruction groups ($p>0.05$). The only significant change was observed at the adjacent level in flexion extension loading condition. The normalized-to-intact ROM at C_6C_7 level in these two reconstruction conditions was significantly higher than that was detected in diskectomy condition ($p<0.05$). Similar to the operative level ROM, the trends under this biomechanical loading mode failed to reach statistical significance secondary to specimen variability and high standard deviations.

The greatest differences between the intact spine and three treatment groups were detected during flexion/extension loading. The fundamental trend in each loading condition demonstrated the diskectomy condition as producing, as expected, an increase in segmental motion. Reconstruction using the PEEK artificial disc restored motion to near intact levels. The final reconstruction using the anterior plate-cage construct reduced motion at the operative level. These reductions in segmental motion, however, were not as low as expected. These findings are attributable to the instability created by the diskectomy condition and follow patterns similar to previous biomechanical studies using anterior plate and interbody cages.

2.1.7 Pilot functional animal study

Using an *in-vivo* goat model, evaluation of implant osseointegration and biocompatibility properties of HA coated and uncoated devices was performed. These properties were radiographically and histologically evaluated at three months post-operatively. Mature female crossbred goats served as the experimental model in this pilot study as these animals are gentle, easy to care for and represent excellent models for cervical spine procedures. There were n = 4 animals for the HA coated and uncoated groups. Following the three month sacrifice, the operative cervical motion segments were sagittally sectioned along the geometric centerline of the implanted device using a Beuhler Isomet saw. Histologic preparation of all samples included dehydration in 100% ethanol, staining using the Villanueva Osteochrome Bone Stain, undecalcified solution processing and embedding in polymethyl-methacrylate (PMMA). Using the EXAKT Microgrinding Device, the embedded specimens were cut at 250 to 300 um thick, ground and polished to 75 um. Microradiographs were obtained of the slide-mounted specimens using Faxitron radiography. The slides were placed twelve inches from the beam and exposed for two minutes, using a technique of 45 kVp and 3mA while in direct contact with the single emulsion high-resolution graphics arts film. For all animals, the soft tissue organs and structures were resected, sectioned and prepared by a veterinarian pathologist. The specimens were fixed in a 10% formalin solution, underwent routine paraffin processing and slide preparation. Using thin-sectioning microtomy, the paraffin embedded sections were cut (3-5µm in thickness), slide mounted and stained using standard Hematoxylin and Eosin (H&E). The spinal cord and local tissue overlying the anterior aspect of the C_3-C_4 operative disc level were evaluated using routine H&E and Macrophage Staining Method (HAM-56). The use of this staining method highlights the presence of activated macrophages within the local tissues. Using plain and polarized light microscopy, histopathological readings of the slide-mounted tissue sections, activated macrophages, presence of wear debris as well as any signs of foreign body giant cells, granulomas inflammatory reactions, degenerative changes or autolysis could be discerned.

All operative cervical motion segments were examined for gross evidence of infection and local pathologic response at the time of necropsy. There was no apparent infection in any of the operative C_3-C_4 levels or adjacent motion segments. Based on gross examination at the time of necropsy, the local tissues from all animals were considered unremarkable and without evidence of ectopic bone formation or other significant histopathologic changes.

Histopathological interpretation of the slide-mounted undecalcified specimens indicated no evidence of significant pathological changes in tissues within or surrounding the specimens. For the HA coated group, there was good intercalation of cancellous bone with the Ti fixation cams and bone apposition to both endplates of the devce (Figure 5). For the

Fig. 5. Left - Good bone apposition to the HA coated devices was seen. Fibrous membranes are around the edges of both components where there is no coating applied, but there is no significant fibrosis at the bone/implant interface. Right – mostly fibrous tissue surrounded the uncoated devices. For all devices, no significant particles of debris were evident.

uncoated group, only focal bone ingrowth to the Ti cam's was noted, with no bone apposition to the PEEK, consistent with the relatively inertness of the material not allowing for bone apposition. For all groups, plain and polarized light microscopy of local tissues overlying the operative sites from experimental levels of both groups indicated a mild inflammatory reaction. The histiocytic infiltration responses were considered secondary to the surgical procedure and healing response. The spinal cord sections exhibited no significant pathological changes based on plain and polarized review. There was no evidence of giant cell reaction or other significant pathological changes, no debris associated with the device, aggresive inflammatory reactions, degenerative changes or autolysis noted.

2.2 PEEK nucleus replacement device

The PEEK nucleus replacement device is a two-piece implant comprised of a top and a bottom plate, with an inner ball and socket articulation (Figure 6). Since PEEK is radiolucent, tantalum (Ta) markers are used to facilitate the visualization of the device location when using radiographic methods. The articulation allows for rotational motions along all three major axes. The motion of the device in axial rotation is unconstrained, while the motions in flexion/extension and lateral bending are semi-constrained slightly beyond the physiological ROM. Similar to all nucleus replacement devices and unlike a total disc replacement, the device ranges of motion are largely dependent upon the constraints from the adjacent tissues, and is designed to restore or maintain the load sharing capabilities of the index disc.

Fig. 6. PEEK nucleus replacement device.

2.2.1 Axial static and fatigue strength

To determine the static and fatigue strength of the device, the smallest footprint (11x20 mm) and height (8 mm) was utilized. These were considered the worst-case scenario for contact stress distribution. The specimens tested were representative of the smallest true contact stress area for all current designs. Testing was performed on an MTS 858 Mini-Bionix II test frame with steel fixturing. A sample size of 3 was used for the static tests with a displacement rate of 2 mm/min. The acceptance criteria was an offset yield load of greater than 2200 N (Lowe, 2004) for the axial static testing. For the fatigue tests, a sample size of 6 was used with a runout load criteria of 3000 N to 5 million cycles (FDA guidance), with R=10 at 10 Hz.

The results of the axial static testing showed that the mean offset yield was 10868 ± 413 N. The primary failure mode was excessive plastic deformation of the top component of the device. For the axial fatigue test, two specimens were tested at a peak compressive load of 9238 N with both failing within 200 cycles due to excessive plastic deformation of the top component, similar to the axial static testing. Two other specimens ran out to 10 million cycles at a peak compressive load of 8151 N. However, upon visual inspection, fatigue cracks emanating from the radiographic marker hole were discovered. Therefore, the load was dropped down to 7065 N for an addition two samples, with a successful outcome. This represented 85%, 75% and 65% of the mean offset yield compressive load, respectively. These results are thought to be well beyond those of the expected *in vivo* physiological loads, and therefore failure was not expected to occur in either static axial compression or dynmaic axial compression.

2.2.2 Shear fatigue strength

To determine the static and fatigue strength of the device, the smallest footprint (11x20 mm) and height (8 mm) was utilized. The specimens tested were also representative of the smallest true contact stress area for all current designs. Testing was performed on an MTS 858 Mini-Bionix II test frame with steel fixturing. A shear angle of 15° was selected based

upon a review of the relevant literature. Extreme flexion of the lumbar spine appears to be approximately 10° on average, with slightly more at the levels L_2L_3 to L_4L_5 and slightly less at L_1L_2 and L_5S_1 when measured *in vivo* (Pearcy, 1984). Therefore, a 15° angle was considered to be at the physiological extreme. Two specimens were used to characterize the shear fatigue strength of the device.

Given the compressive loads obtained during the axial testing, only shear fatigue testing was performed. The two test specimens were successfully tested to 10 million cycles at 6600 N. There is limited data on flexion fatigue testing of human cadaveric lumbar motion segments. The available data states that fatigue failure can occur on average at 263 ±646 cycles with 9 kg of cyclic loading (representing a peak load of 3150 N) at 6° of flexion (Gallagher, 2005). It was therefore thought that the device has adequate compressive-shear fatigue strength for its intended application.

2.2.3 Wear testing and wear particulate characterization

All implants used for wear testing were applicable to a clinical setting and were of the smallest height (8 mm) and footprint (11x20 mm) available. Three separate groups of six implants each were utilized in this wear study. Table 2 summarizes the test methodology. The peak compressive load of 1024 N was chosen based upon the physiological load sharing expected of nucleus replacement devices. The peak compressive load of 2000 N represents a worst case scenario in the event that the device must support the entire compressive load on the anterior column. Group 2 was exposed to 200 kGy of gamma radiation followed by simulated aging. The simulated aging process was similar to ASTM F2003-02, which was developed to measure accelerated aging of UHMWPE in air at 70° C and 5 atm of oxygen, except that the aging time was extended from 14 days to 40 days. All implants were pre-soaked in test fluid for at least 6 weeks. All groups were tested on a six-station spine wear simulator (EndoLab GmbH). The testing fluid consisted of newborn calf serum diluted with phosphate buffered saline (PBS) to a final protein content of 20 g/L. Ethylene-diamine tetraacetic acid (EDTA) was added to the serum at a concentration of 20 mM to bind the calcium ions present in the serum. EDTA is a known preservative, and together with the low protein content and PBS, the addition of sodium azide or other anti-bacterial agent was not used. The test fluid temperature was kept at 37 ± 3° C. Although not part of the test methodology, group 2 was temporarily stopped at 5 million cycles due to simulator availability whereupon the implants were immersed in saline at 37 ± 3° C for 33 weeks. Although unintended, this represented an additional test parameter. The test was subsequently resumed until 10 million cycles was reached. Unloaded soak controls were used for all groups to account for moisture uptake. Group 3 was tested at approximately double the compressive load. The tests were stopped at half million-cycle intervals to clean, dry and gravimetrically assess the wear rates. The average wear rates were determined using linear regression analysis with one-way-analysis-of-variance (ANOVA) used to determine if significant differences ($p < 0.05$) in the wear rates was present. The proteinacious test serum containing PEEK wear debris underwent enzymatic digestion (5x Trypsin digestion and 1.5 mg/mL of Proteinase K per sample at 37° C for 24 hours) followed by a mild acid treatment (10% HCl at 37° C for 24 hours), meeting or exceeding similar protocols previously established to be equivalent for acid and base digestion (Niedzwiecki, 2001). The particles were then analyzed by SEM analysis and characterized

according to their equivalent circle diameter (ECD), aspect ration (AR), roundness (R) and form factor (FF) in accordance with ASTM F 1877-05.

All implants for each group maintained full functionality throughout each test duration with visual and light microscopy revealing no evidence of gross deformation, delamination or fatigue cracks. Since group 1 desplayed a wear-in period from 0-1.0 million cycle, the wear rates were calculated from 1 million cycles on for all groups. For group 1, the wear rate was calculated to be 0.41 ± 0.01 mm^3/million cycles. For group 2, the wear rate was calculated to be 0.52 ± 0.02mm^3/million cycles. For group 3, the wear rate was calculated to be 0.92 ± 0.01 mm^3/million cycles, which was significantly higher than groups 1 and 2. This increase in the wear rate was to be expected, given that the peak compressive load was increased from 1024 N to 2000 N. Overall, the wear rates are less than contempary lumbar total disc arthroplasty devices, which can range from 2.8 to 20.4 mm3/million cycles (Bushelow, 2007; Nechtow, 2006; Grupp, 2009) (Figure 7). The particle analysis conducted via SEM revealed that group 1 had the smallest particulate of 1.09 μm, followed by groups 2 and 3 at 1.71 μm and 1.86 μm respectively. Other than the aspect ratio for group 1, the morphology of the wear particulate appears to be similar for all the groups tested (Figure 8). Using standard nomenclature for describing particle morphology in accordance with ASTM F1877-05, the larger particulate tended to be mostly somewhat roughened or smooth flakes, with some shards and globular particles, along with a few fibrils. Any submicron particulate was smooth, with spheroidal granules.

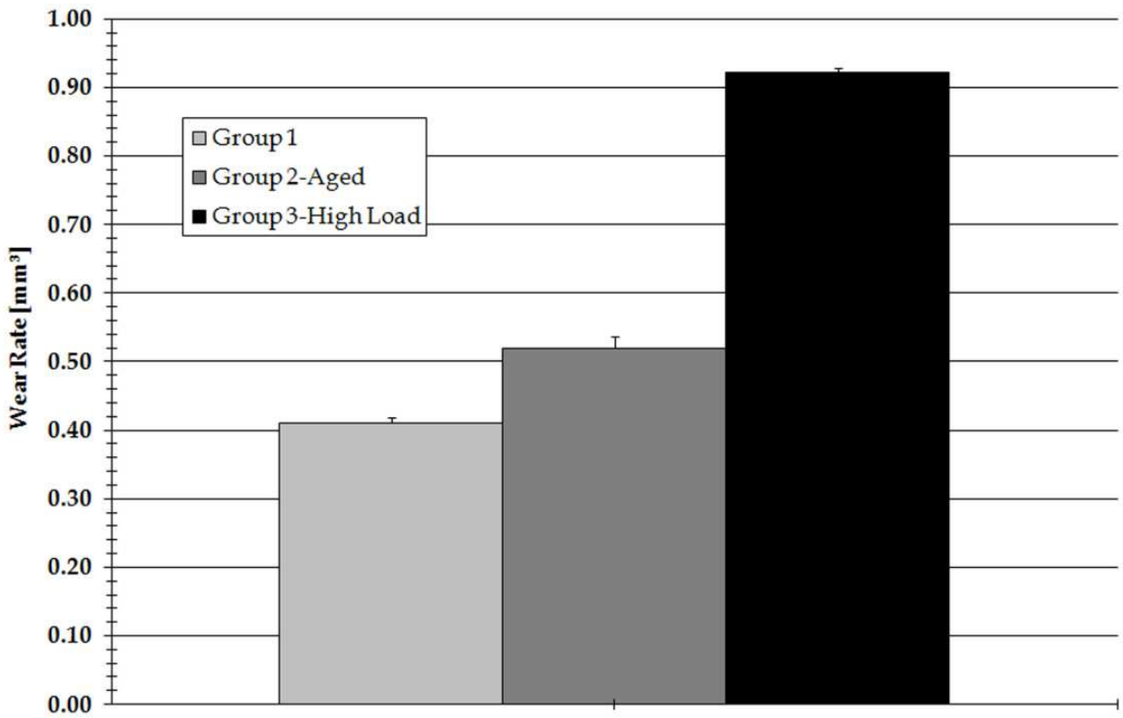

Fig. 7. Average wear rates for the PEEK nucleus replacement device.

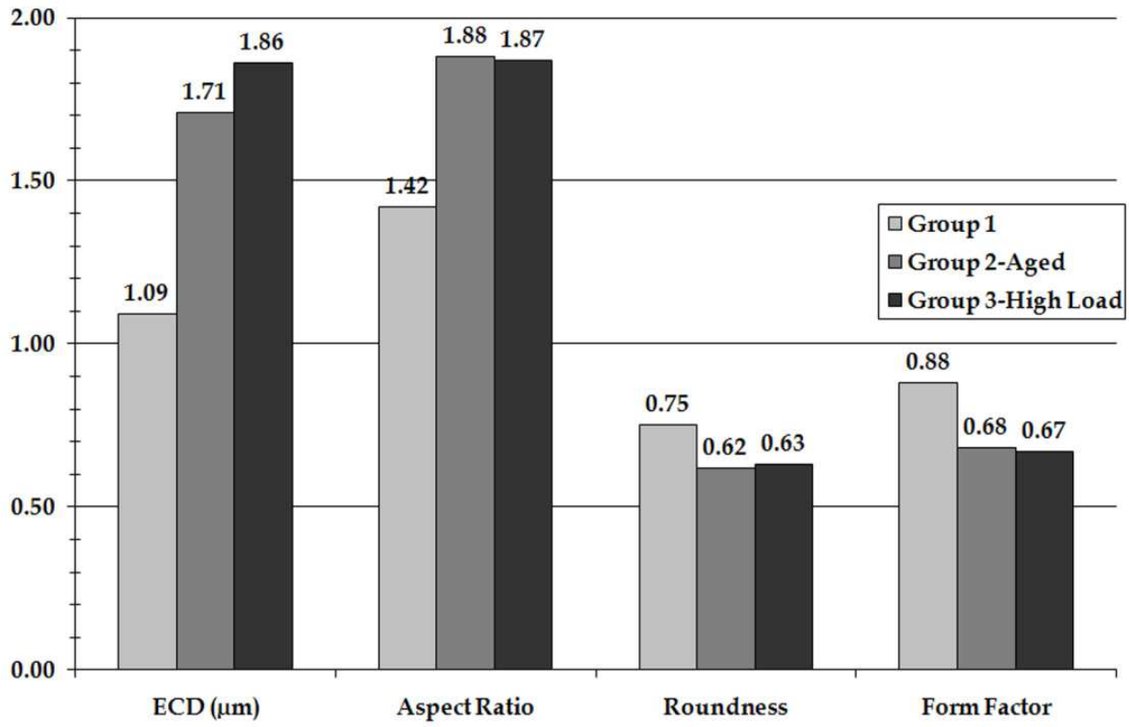

Fig. 8. SEM analysis of the PEEK particulate generated from the wear tests.

2.2.4 Biomechanical analyses

The first study sought to assess the restoration of disc height, the potential adverse effects of the device on the underlying vertebral endplate under physiological loading conditions and an initial assessment of the extrusion risk. A total of eight fresh-frozen human lumbar functional spinal units (L_2L_3 and L_4L_5) were harvested en-bloc and utilized in this investigation. Prior to biomechanical analysis, standard anterior/posterior and standard lateral plain films were obtained to exclude specimens demonstrating intervertebral disc or osseous pathology. Bone mineral density (BMD) scans (DEXA) were performed to exclude specimens demonstrating BMD's less than 0.9 g/cm^3. Each test specimen consisted of two contiguous functional spinal units (three vertebra and two intervertebral discs). One intervertebral disc served as a control and the other intervertebral disc was implanted with the device. To determine restoration of disc height, a 1200 N compressive load was applied. An annular incision followed by a box cut (6 mm x 10 mm) was created on the anatomic right, followed by a complete nucleotomy. A fatigue test was conducted under a left lateral bending moment ranging from 2.5 to 7.5 Nm (250 to 750 N compressive load offset 10 mm). The test was run at 2 Hz for 100,000 cycles. The left lateral bending mode represented a "worst case" scenario with regards to implant extrusion. Upon completion of the biomechanical analyses, each specimen was radiographed and examined for possible fractures and/or migration. Segments were then dissected transversely through the intervertebral discs. Both the intact and implanted discs were examined macroscopically for potential changes. Photographs of the disc were taken using a macro lens to document the condition of the endplates and the annulus. The L1 and L4 vertebrae were scanned on a mCT 80 (ScancoMedical AG, Bassersdorf, Switzerland) to examine the trabecular bone for

potential fractures. The specimens were scanned with an x-ray energy of 70Kvp and current of 114 mA and at an isotropic voxel resolution of 74 microns (image matrix of 1024 x 1024). A total of 500 projections over 180 degrees were collected for each vertebra. An integration time of 700 ms/projection was used, which resulted in a scan-time of about 2.5 - 3 hours/specimen. A repeated measures ANOVA was used to examine differences in ROM between intact, discectomy, and implant conditions. Implant extrusion was assessed by direct observation made from the pre and post fatigue radiographs. Gross macroscopic fractures were determined from the dissection and radiographs for both the control and surgical levels. The microCT images were analyzed by a board certified radiologist (Medical Metrics, Inc. Houston, Texas, USA). The disc height of 2.2 ± 0.6 mm after discectomy significantly decreased ($p<0.05$) to 3.7 ± 1.1 mm for all specimens in comparison to the intact condition under 1.2 kN of compressive loading. Implantation of the nucleus device significantly increased ($p<0.05$) the disc height to 2.6 ± 0.7 mm compared to the discectomy condition. There was no significant difference between the intact and implanted conditions. There were no gross endplate fractures observed at the completion of 100,000 cycles of lateral bending. The evaluation of the microCT images noted no fractures in the endplates or vertebral bodies. There were slight migrations of the device towards the annulotomy, but no extrusions noted.

The second study performed was to quantify the ROM and destructive load to failure properties of the device. A total of eight fresh-frozen human lumbar functional spinal units (L_2L_3 and L_4L_5) were harvested en-bloc and utilized in this investigation. Prior to biomechanical analysis, standard anterior/posterior and lateral plain films were obtained to exclude specimens demonstrating intervertebral disc or osseous pathology. BMD scans using DEXA were performed to exclude specimens demonstrating BMD's less than 0.9 g/cm^3. To determine the multidirectional flexibility, six applied pure moments of ± 7 Nm (flexion and extension, left and right lateral bending, and left and right torsion) were applied to the superior end of the vertically oriented specimen while the caudal portion of the specimen remained fixed to a testing platform. Following the intact analysis, an annular incision followed by a box cut (10 mm x 10 mm) was created on the anatomic left, followed by a complete nucleotomy. After biomechanical testing of the destabilized condition, the nucleus device was implanted and the operative motion segment retested. As a final test, the reconstructed specimen was destructively evaluated under axial compression. Biomechanical data was normalized to the intact condition and expressed as mean ± one standard deviation, with a Repeated Measures Analysis of Variance (ANOVA) and Student-Newman-Keuls test to determine differences among individual groups ($p<0.05$).

Multidirectional flexibility testing indicated significant increases in the segmental range of motion and neutral zone secondary to the annulotomy/nucleotomy procedures after reconstruction of the operative segment. For both calculated parameters, the segmental rotation increased for the destabilized condition versus the intact and reconstructed specimens ($p<0.05$). Importantly, the neutral zone, an indicator of spinal stability of the reconstructed segment, returned to levels not statistically different from the intact condition. As a final test, the reconstructed specimens were destructively evaluated under axial compression. In all specimens except one, the observed failure mechanism was fracture of the vertebral body, without significant disruption of the vertebral endplate. The primary mode of fracture was through the vertebral bodies above and below the operative disc level. The mean failure load was 3340 ± 2029 N. This average fracture load is comparable to the compressive failure load for intact lumbar segment (Lowe, 2004).

2.2.5 Functional animal study

Evaluation of the mechanical behavior and elicited histopathological response following long-term implantation in a functional animal (baboon) model of the device was performed. Fourteen mature male baboons (Papio cynocephalus) were randomized into two post-operative time periods of six-months (n=7) and twelve-months (n=7). Each animal underwent a lateral transperitoneal surgical approach followed by complete nucleotomy at L_3-L_4 and L_5-L_6 levels. The inferior L_5-L_6 level was reconstructed using the nucleus replacement device while the adjacent level served as a control.

Analyses were based on gross necropsy, MRI radiography, plain X-ray, microradiography, and biocompatibility assays (local and systemic histology) performed at the six and twelve month post-operative time-points. resected, sectioned and prepared by a veterinarian pathologist. The specimens were fixed in a 10% formalin solution, underwent routine paraffin processing and slide mounting. Using thin-sectioning microtomy, the paraffin embedded sections were cut (3-5μm in thickness), slide mounted and stained using standard Hematoxylin and Eosin (H&E). The spinal cord sections, obtained from each operative disc level, were evaluated using routine H&E. The local tissues overlying the operative levels underwent the following immunocytochemistry analyses using standard immunocytochemistry techniques, including primary and secondary antibodies combined with the avidin-biotin complex (ABC)-horseradish peroxidase. Immunohistochemical localization of intracellular and membrane bound macrophage expressing cytokines included IL-1, IL-2, IL-6 and Tumor Necrosis Factor-Alpha and beta (TNF-α,β). The Macrophage Staining Method (HAM-56) was used to highlight the presence of activated macrophages within the local tissues. Using plain and polarized light microscopy, histopathological readings of the slide-mounted tissues, activated macrophages, presence of wear debris as well as any signs of foreign body giant cells, granulomas inflammatory reactions, degenerative changes or autolysis could be discerned. Pathological assessment for all systemic and local tissues included, but was not limited to, the architecture of the tissues, presence of wear debris as well as any signs of foreign body giant cell / granulomas inflammatory reactions, degenerative changes or autolysis.

Multidirectional flexibility testing indicated no difference in axial rotation ($p>0.05$) for the six-month groups, comparing the intact spine to surgical motion segments. Flexion/extension and lateral bending exhibited reduced segmental motion for the nucleus replacement device and operative control levels at six months versus the non-operative intact spine ($p<0.05$). However, these findings were also noted in the operative control levels demonstrating the effect of surgical intervention itself on segmental stability. At twelve months, segmental motion was restored to the intact levels for the reconstructed levels ($p>0.05$). Histopathologic analysis of the nucleus replacement treatment exhibited increased densification of trabeculae along the endplate periphery, which corroborated with Modic Type I changes observed with MRI and radiographically. Evidence of implant subsidence was noted in 5/7 cases at six months and 7/7 cases at twelve months, which correlated with the absence of articular cartilage in some regions. A limitation of this study was the use of a single height nucleus replacement device for all treated discs. This resulted in difficulties in insertion and placement of the device and significant over distraction of the disc space. The difficulties in insertion and over distraction may have resulted in the use of more force for proper placement. This potentially induced endplate damage at the treated disc levels and led to abnormal high contact stress on the endplates, which may have been the precursor to the Modic changes and subsidence. Plain and polarized light microscopy of local tissues overlying the operative sites from both the experimental and control levels indicated a

chronic inflammatory reaction, with evidence of fibrous connective replacement and infiltration of mononuclear cells. These observations were considered secondary to the surgical procedure and, importantly, occurred at both the control and experimental operative levels. There was no evidence of cellular apoptosis, giant cell reaction or other significant pathological changes. Analysis of the immunohistochemical antibody stains for the local tissues overlying the experimental and control levels were negative in each case. In the histological analyses, there was no detectable wear debris from the device and no evidence of an osteolytic response. There was no evidence of a pro-inflammatory cytokine reaction at any of the experimental or control levels.

3. Clinical summary

Worldwide clinical usage of both devices is ongoing. Currently, there have been no reported adverse events due to a material failure, such as device breakage, fatigue failure or an aggressive host immune response leading to a revision surgery to remove the device. Clinical results as measured by validated measures such as Oswestry Disability Index (ODI) and Visual Analog Scale (VAS), along with patient satisfaction, suggest that both devices can relieve the symptoms of their respective degenerative processes (Figures 9, 10). From a biomaterial perspective, no adverse events have occurred as a direct result of these devices not performing as expected. Based upon worldwide clinical success, and the success of a US pilot IDE study, the nucleus replacement device was granted approval by FDA to start a first of its kind IDE pivotal study in the US.

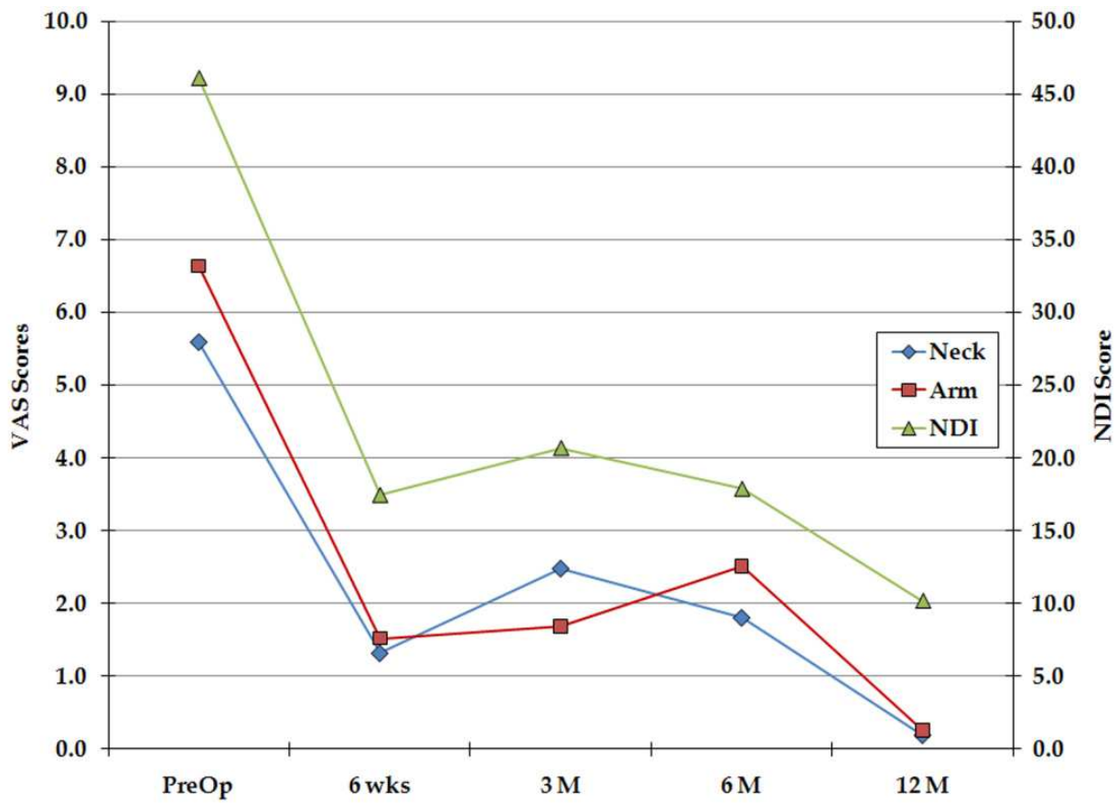

Fig. 9. ODI and VAS scores from the worldwide usage of the cervical arthroplasty device.

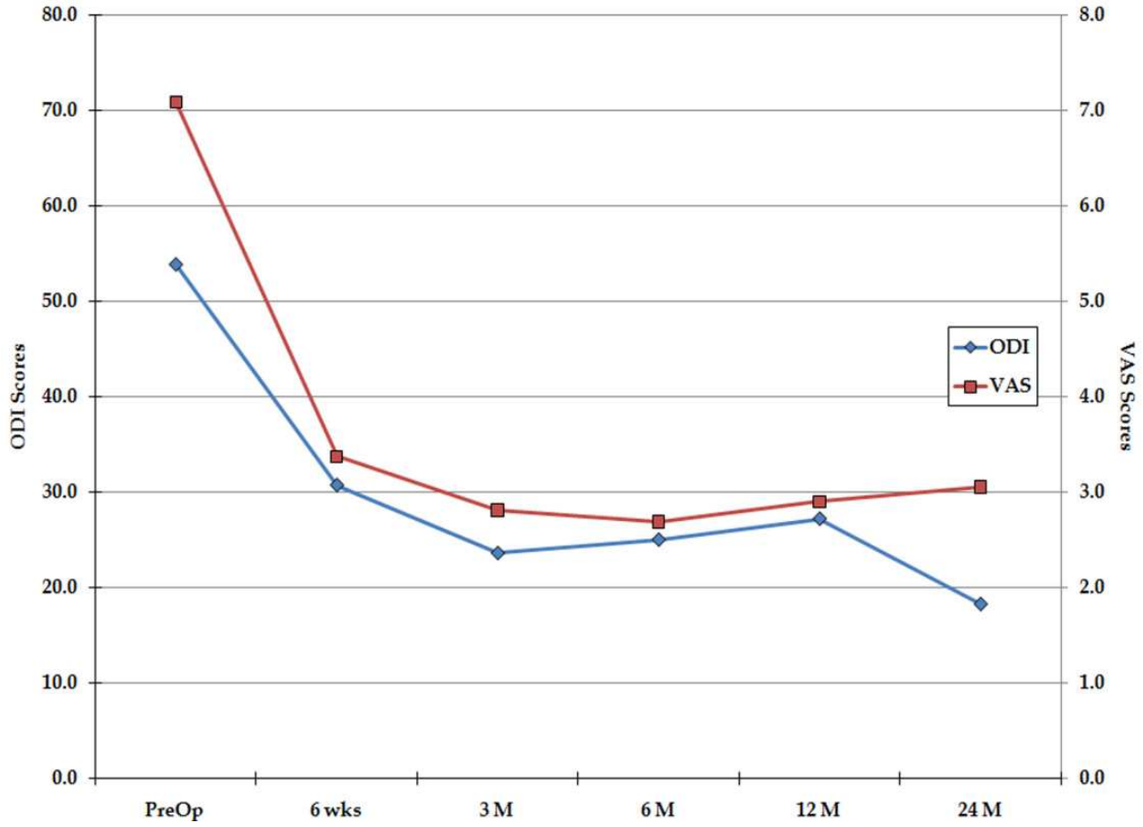

Fig. 10. ODI and VAS scores from the US IDE pilot study for the nucleus replacement device.

4. Conclusion

The concept of reconstruction of the lumbar and cervical disc is not new, as clinical experimentation goes back to the early 1950's. Since then, the scientific and clinical community has sought to improve upon the selection of available biomaterials for use in the disc arthroplasty arenas. The mainstay of these materials has been ceramics, metal alloys and polymers, in large part due to the history gained form their use in total joint reconstruction. Currently there is no universal material that is considered the ultimate biomaterial, and an in-depth knowledge of a given material is important in understanding and predicting its response when used in an application as demanding as an implantable biomaterial. Knowledge can be gained by not only performing the appropriate testing on the bulk properties of the material, but also proper preclinical testing of the constructed device. More importantly, adroit interpretation of these results is fundamental to the clinical success of the device (Fraser, 2004; Kurtz, 2009). The use of PEEK in spinal arthroplasty represents a new application of this material. Although the history of PEEK suggests that it has the necessary material properties to serve as a long-term implantable arthroplasty material, it's use in the form of any arthroplasty device has not been diligently explored. Therefore, a battery of preclinical testing was performed, and the interpretation of the results for both a cervical disc arthroplasty device and lumbar nucleus replacement device have allowed for successful advancement to the clinical usage. The results of these

combined preclinical studies described can be used in an ongoing basis to further analyze the use of PEEK in arthroplasty applications. Long term clinical follow up is needed to further support the preclinical results.

5. Acknowledgment

The authors would like to acknowledge Nathaniel Ordway at SUNY Upstate New York for help with conducting the biomechanical studies, along with Bryan Cunningham of Union Memorial Hospital for help with conducting the biomechanical and animal studies. The authors would also like to acknowledge Dr. Nadim Hallab of Bioengineering Solutions for performing the particulate analyses, along with Markus W. Wimmer and Thorsten Schwenke at RUSH Medical Center for help in conducting the wear studies.

6. References

Balsano, M.; Zachos, A. & Ruggiu A. (2011). Nucelus desc arthroplasty with the NUBAC device: 2-year clinical experience. *Eur Spine J*, Vol. 20, Suppl 1 (May, 2011) pp. S36-40 ISSN 0940-6719

Bergen, H. (2011). The Norwegain Arthroplasty Register, In: Centre of Excellence of Joint Replacements, 07.07.2011, Available from http://nrlweb.ihelse.net/eng/Report_2010.pdf

Bushelow, M.; Walker, J. & Coppes J. Comparison of Wear Rates: Metal/UHWMPE and Metal-on-Metal Total Disc Arthroplasty. Trans 22nd (2007) NASS p32

Cavanaugh, D.; Nunely P. & Kerr J. (2009). Delayed Hyper-reactivity to Metal Ions After Cervical Disc Arthroplasty: A case report and literature review. *Spine*, Vol. 34, No. 7 (April, 2009) E262-265 ISSN 0362-2436

Cunningham, B.; Hu, N. & Zorn, C. Comparative fixation methods of cervial disc arthroplasty versus conventional methods of anterior cervical arthrodesis: serration, teeth, keels, or screws? *J Neurosurg Spine*, Vol. 12, No. 2 (February, 2010) pp. 214-220 ISSN 1547-5654

Devin, C.; Myers, T. & Kang J. (1889). Chronic failure of a lumbar total disc replacement with osteolysis. Report of a case with nineteen year follow up. *J Bone Joint Surg Am* Vol.90, No. 10 (October, 2008) pp. 2230-2234 ISSN 0021-9355

Francois, J.; Coessens, R. & Lauweryns P. (2007). Early removal of a Maverick disc prosthesis: surgical findings and morphological changes. *Acta Orthop Belg*, Vol. 73, No. 1(2007) pp. 122-27 ISSN 0001-6462

Fraser, R.; Ross, E. & Lowery G. (2004) AcroFlex design and results. *Spine J* Vol. 4, No. 6 Suppl (Nov-Dec, 2004) pp. 245S-51S 1529-9430

Gallagher, S.; Marras, W. & Davis, K. (2005) Torso Flexion Load and the Fatigue Failure of Human Lumbosacral Motion Segments. *Spine,* Vol. 30, No. 20 (October, 2005) pp. 2265-73, 2005 ISSN 0362-2436

Garellick, G; Darrholm J & Rogmark C. (2010). The Swedish Hip Arthroplasty Register, In: Swedish Hip Arthroplasty Register, Annual Report 2008, 07.07.2011, Available from https://www.jru.orthop.gu.se/

Grupp, T.; Yue, J. & Garcia R. (2008) Biotribological evaluation of artificial disc arthroplasty devices: influence of loading and kinematics patterns during in vitro wear simulation. *Eur Spine* J Vol. 18, No.1 (January, 2009) pp. 98-108 ISSN 0940-6719

Guyer, R.; Shellock, J & MacLennan, B. (2011). Early failure of metal-on-metal artificial disc prostheses associated with lymphocytic reaction: diagnosis and treatment experience in four cases. *Spine*, Vol. 36, No. 7, (April, 2001) E492-497 ISSN 0362-2436

Kurtz, S. & Devine J. (2007). PEEK biomaterials in trauma, orthropedic and spinal implants. *Biomaterials*, Vol. 28, No. 32, (November, 2007) pp. 4845-4869 ISSN 0142-9612

Kurtz, S. MacDonald, D. & Ianuzzi, A. (1976). The natural history of polyethylene oxidation in total disc replacment. *Spine*, Vol. 15, No. 34, (October, 2009) pp. 2369-2377 ISSN 0362-2436

Licina, P. & Thorpe P. (1948). Osteolysis and complications associated with artificial disc replacement. *J Bone Joint Surg,* Vol. 86-B, Suppl IV (2004) pp. 460-461 ISSN 0301-620X

Lowe, T.; Hashim, S. & Wilson, L. (1976). A biomechanical study of regional endplate strength and cage morphology as it relates to structural interbody support. *Spine*, Vol. 1, No. 29, (Novermber, 2004) pp. 2389-2394 ISSN 0362-2436

Moroney, S. Schultz, A. & Miller J. (1988). Analysis and measurement of neck loads. *J Ortho Res*, Vol. 6, No. 5, (September, 1988) pp. 713-720 ISSN 1554-527X

Murrey D.; Janssen M & Delamarter R. (2009). Results of the Prospective, Randomized, Controlled Multicenter Food and Drug Administration Investigational Device Exemption Study of the ProDisc-C Total Disc Replacement Versus Anterior Discectiomy and Fusion for the Treatment of 1-level Symptomatic Cervical Disc Disease. *The Spine Journal,* Vol.9, No. 4, (April, 2009) pp. 275-286 ISSN 1529-9430

Nechtow, W.; Hinter, M. & Bushelow M. IVD Replacement Mechanical Performance Depends Stronlgy on Input Parameters. Trans 52nd ORS (2006) p0118.

Niedzwiecki, S.; Klapperich, C, & Short J. (2001). Comparison of three joint simulator wear debris isolation techniques: acid digestion, base digestion, and enzyme cleavage. *J Biomed Mater Res* Vol. 56, No. 2, (August, 2001) pp. 245-249 ISSN 1549-3296

Pearcy, M.; Portek, I. & Shepherd J. (1976). Three-Dimensional X-ray Analysis of Normal Movement in the Lumbar Spine. *Spine*, Vol. 9, No. 3 (April, 1984) pp.294-297 ISSN 0362-2436

Panjabi, M.; Crisco, J. & Vasavada A. (2001) Mechanical Properties of the Human Cervical Spine as Shown by Three Dimensional Load Displacement Curves. *Spine*, Vol. 26, No. 24 (December, 2001) pp. 2692-2700 ISSN 0362-2436

Przybyla A.; Skrzypeic, D. & Pollintine, P. Strength of the cervical spine in compression and bending. *Spine*, Vol. 32, No. 15, (July, 2007), pp. 1612-1620 ISSN 0362-2436

Rae, P.; Brown, E. & Orler, E. (1960). The mechanical properties of poly(ether-ether-ketone) (PEEK) with emphasis on the large compressive strain response. *Polymer* Vol. 48, No. 2 (January, 2007) pp.598-615 ISSN 0032-3861

Reitman, C.; Mauro, K. & Nguyen. L. (2004). Intervertebral Motion Between Flexion and Extension in Asymptomatic Individuals. *Spine*, Vol. 29, No. 24 (December, 2004) pp. 2832-2843 ISSN 0362-2436

Senegas, J. (2002). Mechanical supplementation by non-rigid fixation in degenerative intervertebral lumbar segments: the Wallis system. *Eur Spine J* Vol. 11, Suppl 2 (October, 2002) pp. S164-169 ISSN 0940-6719

Snijders, C.; Hoek van Dijke, G. & Roosch E. (1991). A biomechanical model for the analysis of the cervical spine in static postures. *J Biomech*, Vol. 24, No. 9, (1991) pp. 783-792 ISSN 0021-9290

Zigler, J.; Delamarter R. & Linovitz R. (2007). Results of the Prosperctive, Randomized, Mulitcenter Food and Drug Administration Investigational Device Exemption Study of the ProDisc-L Total Disc Replacement Versus Circumferential Fusion for the Treatment of 1-Level Degernative Disc Disease. *Spine*, Vol. 32, No. 11, (May, 2007), pp. 1155-1162 ISSN 0362-2436

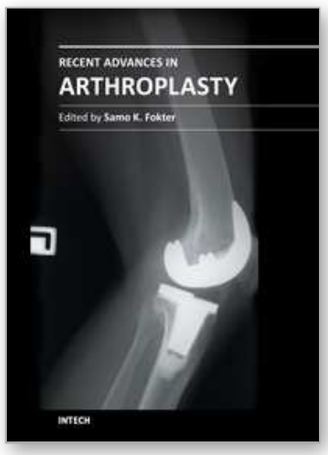

Recent Advances in Arthroplasty

Edited by Dr. Samo Fokter

ISBN 978-953-307-990-5
Hard cover, 614 pages
Publisher InTech
Published online 27, January, 2012
Published in print edition January, 2012

The purpose of this book was to offer an overview of recent insights into the current state of arthroplasty. The tremendous long term success of Sir Charnley's total hip arthroplasty has encouraged many researchers to treat pain, improve function and create solutions for higher quality of life. Indeed and as described in a special chapter of this book, arthroplasty is an emerging field in the joints of upper extremity and spine. However, there are inborn complications in any foreign design brought to the human body. First, in the chapter on infections we endeavor to provide a comprehensive, up-to-date analysis and description of the management of this difficult problem. Second, the immune system is faced with a strange material coming in huge amounts of micro-particles from the tribology code. Therefore, great attention to the problem of aseptic loosening has been addressed in special chapters on loosening and on materials currently available for arthroplasty.

InTech Europe
University Campus STeP Ri
Slavka Krautzeka 83/A
51000 Rijeka, Croatia
Phone: +385 (51) 770 447
Fax: +385 (51) 686 166
www.intechopen.com

InTech China
Unit 405, Office Block, Hotel Equatorial Shanghai
No.65, Yan An Road (West), Shanghai, 200040, China
中国上海市延安西路65号上海国际贵都大饭店办公楼405单元
Phone: +86-21-62489820
Fax: +86-21-62489821

IntechOpen